FACULTY OF ELECTRICAL ENGINEERING
KTE
September 10 - 12, 2007
Pilsen, Czech Republic

NUMERICAL MODELING OF MHD EFFECT FOR PUMPING OF MOLTEN METALS

DR. ING. JIŘÍ BÜLOW, PROF. ING. IVO DOLEŽEL, CSC.
ING. PAVEL KARBAN, DOC. ING. BOHUŠ ULRYCH, CSC.

Abstract: *The paper deals with the numerical modeling of pumping molten metals based on the principle of the magnetohydrodynamic effect, i.e. force effect of an external stationary current field and magnetic field on an electrically conductive liquid. Described is the physical essence of the effect that represents the starting point for the formulation of its mathematical model. The theoretical analysis is illustrated on two examples. The first pump works with practically uniform electric field in a hydrodynamically less favorable channel of rectangular cross-section while the second one with nonuniform electric field in hydrodynamically more advantageous circular channel. The conclusion is devoted to the discussion about the possibilities of optimization of the device.*

Key words: *molten metal, magnetohydrodynamic effect, electric field, magnetic field, numerical analysis*

INTRODUCTION

Electromagnetic pumping or dosing of nonferrous molten metals represents a process based on the effects of electrodynamic forces in melt. The relevant devices differ from one another particularly by the manner how these forces are produced. The main systems work on the electrodynamic and magnetohydrodynamic principles that are described in numerous references (see, for example, [1–3]).

On the other hand, all devices of this kind are characterized by consumption of a considerable amount of energy. Finding of their optimal arrangement is, therefore, a must. But increasing of their efficiency cannot be done without a detailed knowledge of all physical phenomena taking place in them. And this is a relatively complicated business, because from the viewpoint of the mathematical and computer modeling, the process of pumping usually represents a complex coupled problem characterized by the interaction of several physical fields (generally electric field, magnetic field, temperature field, field of flow) and other possible accompanying effects.

The paper is devoted to the verification of possibilities of pumping molten metals based on the principle of the magnetohydrodynamic effect, i.e. force effect of an external stationary current field and magnetic field on electrically conductive liquids. Described is the physical essence of the effect that represents the starting point for the formulation of its mathematical model considered as a coupled electromagnetic-hydrodynamic problem. The theoretical analysis is illustrated on two examples. The first pump works with practically uniform electric field in a hydrodynamically less favorable channel of rectangular cross-section while the second one with nonuniform electric field in hydrodynamically more advantageous circular channel. Both versions are evaluated from the viewpoint of the pumping lead. The conclusion is devoted to the discussion of the possibilities of optimization of the device.

1 FORMULATION OF THE PROBLEM

The principle of the magnetohydrodynamic effect for pumping electrically conductive liquids (including molten metals) is indicated in Fig. 1. The column of liquid **1** is flown through by direct current I_e whose density $\boldsymbol{J}_e$ is a vector parallel to axis x, perpendicularly to the axis of the channel. This current enters and departs the liquid on two (in the case of molten metal) heat-proof electrodes **2** and **3**. The conductors **4** forming a system of saddle coils surrounding the channel carry direct current I_m that produces in the liquid medium stationary magnetic field. The vector of its magnetic flux density $\boldsymbol{B}_m$ is oriented in direction y, that is perpendicular both to the axis of the channel and vector $\boldsymbol{J}_e$. The interaction of the above current and magnetic fields gives rise to the volume Lorentz forces in melt. Their integral value (vector $\boldsymbol{F}_L$) is oriented in direction z and pushes the conductive medium upwards.

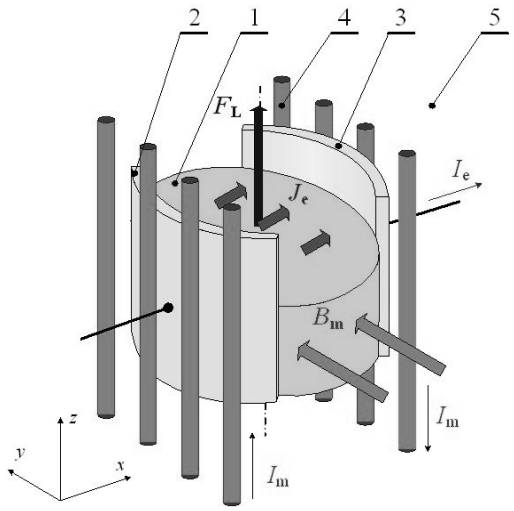

Fig. 1. The principle of a MHD pump for electrically conductive liquids
***1** – electrically conductive liquid*
***2, 3** – heat-proof nonferromagnetic electrodes*
***4** – conductors of the saddle coils*
***5** – ambient air*

In the paper we consider three following arrangements of the pump channel:

a) channel of a rectangular cross-section, the conductors **4** being arranged in plane $x = \text{const}$, see Fig. 2a,

b) channel of a circular cross-section, the conductors **4** being arranged in plane $r = \text{const}$, see Fig. 2b,

c) channel of a circular cross-section, the conductors **4** being arranged in plane $x = \text{const}$, see Fig. 2c,

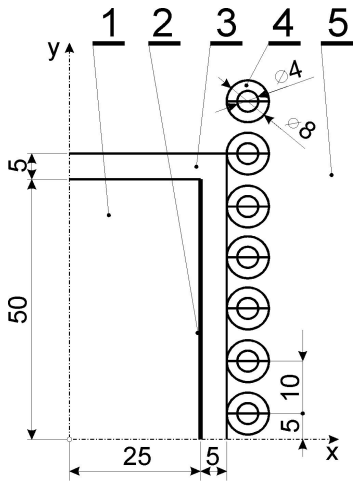

*Fig. 2a. The channel of a rectangular cross-section, the conductors **4** being arranged in plane $x = \text{const}$*

2 MATHEMATICAL MODEL OF THE PUMP

The mathematical model of the investigated MHD pump describes stationary electric and magnetic fields in electrically conductive, Nonferromagnetic liquid medium in channel **1** (Figs. 2a, b, c). If the length of the channel is assumed much larger than its cross-section, the problem can be considered 2D and formulated in Cartesian coordinate system x, y.

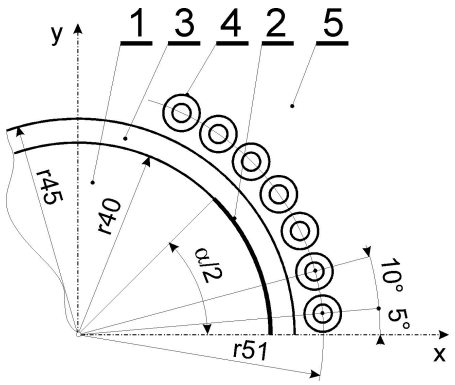

*Fig. 2b. The channel of a circular cross-section, the conductors **4** being arranged in plane $r = \text{const}$*

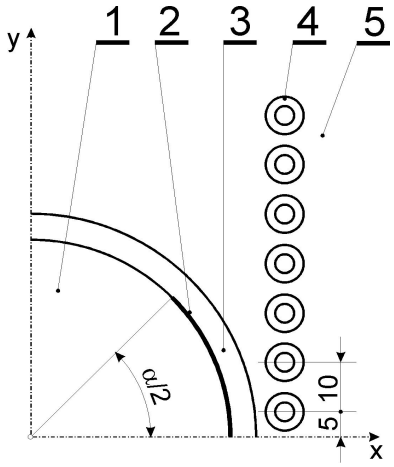

*Fig. 2c. The channel of a circular cross-section, the conductors **4** being arranged in plane $x = \text{const}$*

2.1. The definition area

The definition area of the problem is given by unification of all mentioned subdomains: $\Omega = \Omega_e = \Omega_m =$ **1+2+3+4+5**, see Figs. 2a, b, c. The area is bounded by a fictitious artificial boundary Γ_∞ placed in the air **5**, at a sufficient distance from the channel **1**.

2.1. The differential equations

The *electric field* (see [4], [5]) in the domain Ω_e is described by the Laplace equation for the scalar electric potential $\varphi(x, y)$

$$\Delta\varphi = 0\,. \tag{1}$$

This field produces in electrically conductive liquid **1** in the channel currents of density

$$\boldsymbol{J}_e = \mathbf{i}\cdot J_{ex}(x, y) + \mathbf{j}\cdot J_{ey}(x, y) \tag{2}$$

that is given as

$$\boldsymbol{J}_e = -\gamma_e \cdot \operatorname{grad}\varphi \tag{3}$$

where γ_e is the electrical conductivity of the liquid medium.

The magnetic field (see [4], [5] again) in the domain Ω_m may be described by the magnetic vector potential $\boldsymbol{A} = \mathbf{i}\,0 + \mathbf{j}\,0 + \mathbf{k}\,A_z(x, y)$. In the area of conductors **4** carrying DC current I_m the potential satisfies equation

$$\operatorname{rot}\operatorname{rot}\boldsymbol{A} = \mu_0\,\boldsymbol{J}_m \tag{4}$$

with condition

$$I_{\mathrm{m}} = \int_{S_4} \boldsymbol{J}_{\mathrm{m}} \cdot \mathrm{d}\boldsymbol{S} \tag{5}$$

where S_4 is the cross-section of conductor **4**. Otherwise there holds

$$\mathrm{rot}\ \mathrm{rot}\ \boldsymbol{A} = \boldsymbol{0} \tag{6}$$

Magnetic flux density in this region in the form $\boldsymbol{B} = \mathbf{i} \cdot B_x(x, y) + \mathbf{j} \cdot B_y(x, y)$ follows from relation

$$\boldsymbol{B} = \mathrm{curl}\, \boldsymbol{A}\,. \tag{7}$$

The *resultant Lorentz force* $\boldsymbol{F}_{\mathrm{L}} = \mathbf{i} \cdot 0 + \mathbf{j} \cdot 0 + \mathbf{k} \cdot F_{\mathrm{L}z}$ acting on the liquid medium in space V_1 of channel **1** is then given by relation

$$\boldsymbol{F}_{\mathrm{L}} = \int_{V_1} \left(\boldsymbol{J}_{\mathrm{e}}(x, y) \times \boldsymbol{B}(x, y) \right) \mathrm{d}V\,. \tag{8}$$

The pumping lead h_{L} of the pump (following from the balance of forces) is then given as

$$h_{\mathrm{L}} = \frac{F_{\mathrm{L}z}}{\rho_{\mathrm{m}} g S_1} \tag{9}$$

where ρ_{m} is the specific mass of the liquid medium **1** and S_1 is the cross-section of the channel.

2.3. Boundary conditions

The boundary conditions for both fields (of the first and seconds kinds) follow from the physical context of the problem. The same holds for the interface conditions.

3 COMPUTER MODEL AND ACCURACY OF SOLUTION

The mathematical model described in paragraph 2 was solved numerically by the FEM-based professional code QuickField. Attention was paid to the convergence of solution with respect to the position of the artificial boundary and density of the discretization mesh. In order to obtain three nonzero valid digits for the force $F_{\mathrm{L}z}$ it was necessary that the mesh contained about 120000–150000 nodes, in the dependence on the shape of the channel **1** (see Figs. 2a, b, c).

For an illustration, Fig. 3 shows the calculated distribution of equipotentials and vectors $\boldsymbol{J}_{\mathrm{e}}$ of the current field for the arrangement **a)** and Fig. 4 depicts the distribution of the force lines for the same version. It is obvious that such figures provide sufficient information about the suitability of the corresponding arrangements: the more uniform are both fields and the denser are both systems of the force lines, the higher is the total Lorentz force $\boldsymbol{F}_{\mathrm{L}}$ and pumping lead h_{L}. A more detailed discussion to these aspects is in the following paragraph.

4 ILLUSTRATIVE EXAMPLE

The aim of the presented example is to evaluate three considered arrangements (see par. 1) of the MHD pump from the viewpoint of their pumping lead h_{L} and also other aspects that may (for the particular arrangement) have some influence on this quantity.

4.1. Input data

The arrangement and basic dimensions of all three versions of the pump are obvious in Figs. 2a, b, c.

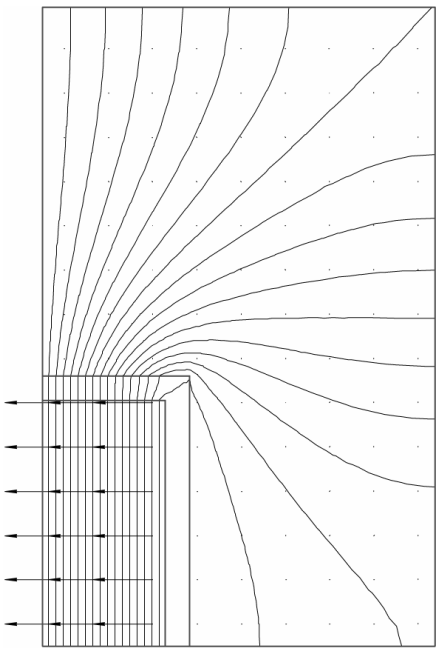

*Fig. 3. Calculated distribution of the equilines and vectors of current density $\boldsymbol{J}_{\mathrm{e}}$ in the cross-section of the channel (version **a**), $a = 0.05$ m, see Fig. 2a)*

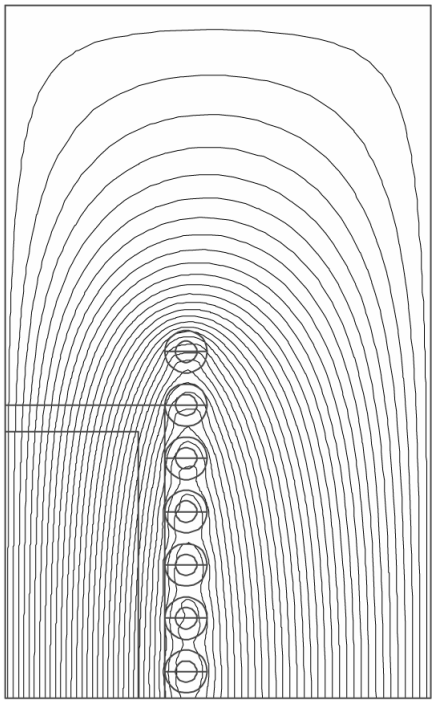

*Fig. 4. Calculated distribution of the force lines in the cross-section of the channel (version **a**), $a = 0.05$ m, see Fig. 2a)*

The cross-section of the channel **1** is in arrangement:
a) $S_1 = ab$, $a = 0.05\,\mathrm{m}$, $b = 0.1\,\mathrm{m}$, $S_1 = 0.005\,\mathrm{m}^2$ (Fig. 2a),
b), c) $S_1 = \pi r_1^2$, $r_1 = 0.04\,\mathrm{m}$, $S_1 = 0.005\,\mathrm{m}^2$ (Fig. 2b, c).

The working height of the channel (height of the channel **1** affected by both electric and magnetic field and Lorentz force $\boldsymbol{F}_{\mathrm{L}}$) $h_1 = 0.1\,\mathrm{m}$ (corresponds to the volume V_1, see (7)).

The physical parameters of particular materials are listed in Tab.1.

Tab. 1. Physical and other parameters of individual parts of the pump

Item	Element	Material	Physical quantities
1	liquid medium	molten Al	$T_{Al} = 930\,°C$ $\rho = 2.375 \cdot 10^3\ kg/m^3$ $\gamma_e = 7.664 \cdot 10^6\ S/m$ $J_e = 5 \cdot 10^5\ A/m^2\ (*)$
2	electrodes	austenitic steel [7]	$\gamma_e = 1.5 \cdot 10^6\ S/m$ $\mu_r = 1$ $I_e = 5 \cdot 10^3\ A\ (**)$
3	shell	molten basalt	$\gamma_e = 12\ S/m$ $\mu_r = 1$
4	hollow conductors	Cu	$r_{max} / r_{min} = 8/4\ mm$ $\gamma_e = 5.6 \cdot 10^7\ S/m$ $J_m = 5 \cdot 10^7\ A/m^2$ $I_m = 5 \cdot 10^3\ A\ (*)$
5	ambient medium	air	$\gamma_e = 0\ S/m$

(*) holds for all arrangements of the pump
(**) holds just for arrangement **a)**

4.2. Results and their discussion

The basic qualitative evaluation of the individual versions of the pump can be carried out (as was said in paragraph 3) on the basis of graphical image of the corresponding electric and magnetic fields.

For example, Figs. 5a, b show the influence of the arrangement (see paragraph 1) of channel **1** on the uniformity of the electric field in the working medium in the pump for the case of the circular cross-section of the channel. The most uniform field we obviously obtain for the arrangement **a)** (Fig. 3) – rectangular channel, while arrangements **b)** and **c)** provide less uniform and practically identical fields.

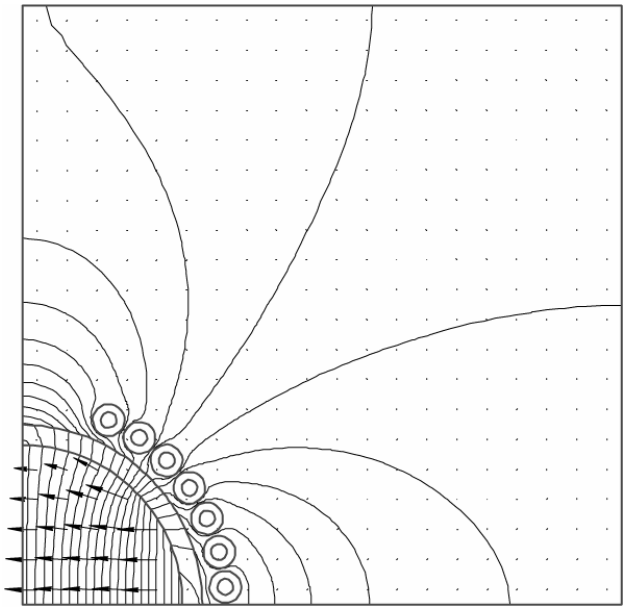

*Fig. 5a. Electric field, arrangement **b)**, $r = const$, $\alpha = 90°$, see Fig. 2b*

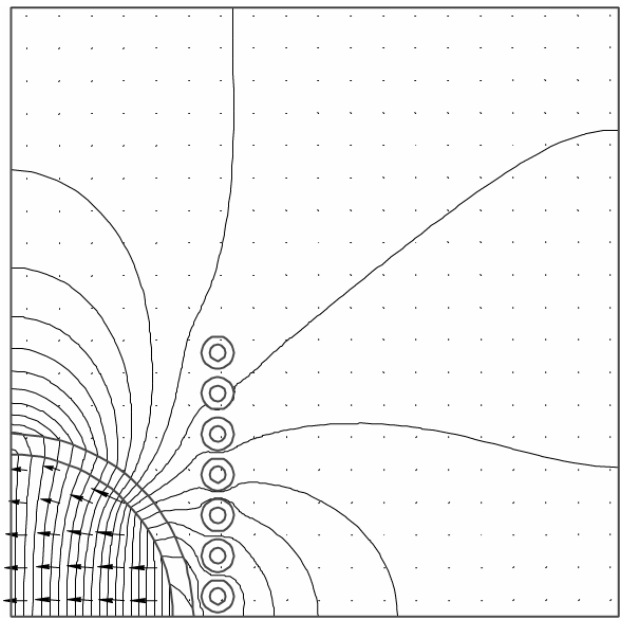

*Fig. 5b. Electric field, arrangement **c)**, $x = const$, $\alpha = 90°$, see Fig. 2c*

Nevertheless, comparison of Figs. 6a (arrangement **b),** Fig. 2b) for $\alpha = 120°$ and 6b for $\alpha = 150°$ indicates, that for some angle $\alpha_{opt} \in \langle 120°,\ 150° \rangle$ we obtain practically uniform electric field.

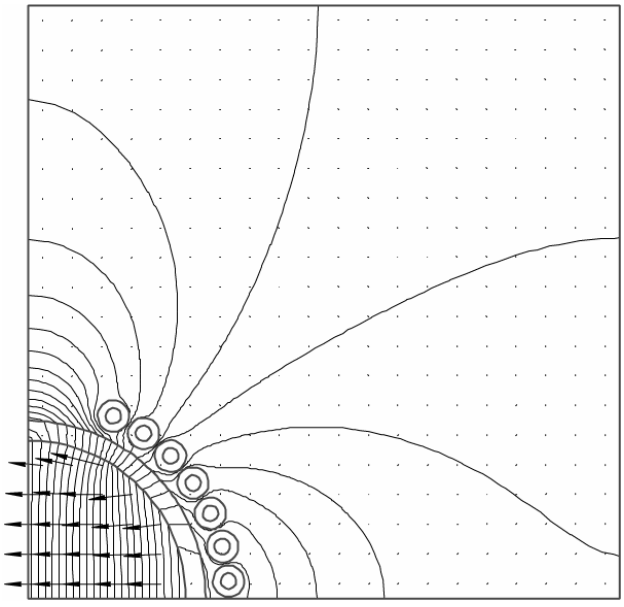

*Fig. 6a. Electric field, arrangement **b)**, $r = const$, $\alpha = 120°$, see Fig. 2b*

On the contrary, comparison of Fig. 4 and 7a, b provides information that there are no practical differences in the uniformity of the magnetic field in channel 1 for all three alternatives **a)**, **b)** and **c)**.

Somewhat more detailed, to some extent quantitative evaluation of the individual versions may be carried out through the analysis of graphs depicting the distribution of vectors $\boldsymbol{J}_e$ and $\boldsymbol{B}$ of the corresponding electric and magnetic fields along the perimeter of the corresponding channel **1** of the pump.

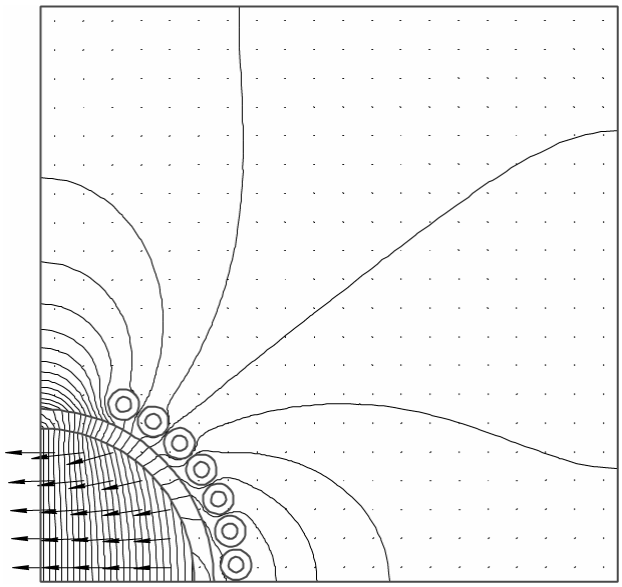

*Fig. 6b. Electric field, arrangement **b)**, $r = const$, $\alpha = 150°$, see Fig. 2b*

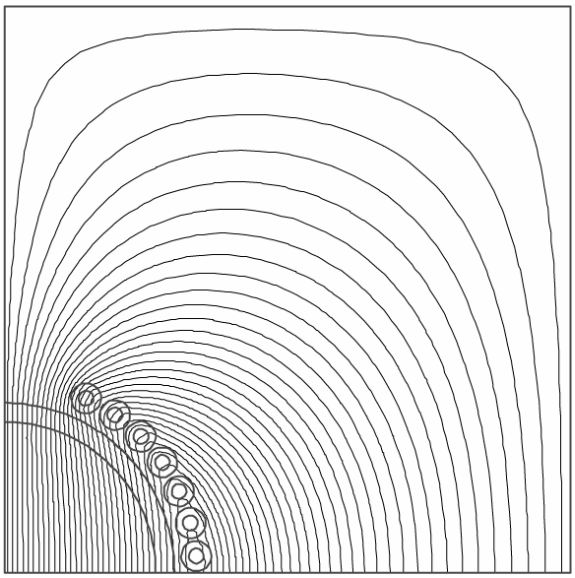

*Fig. 7a. Magnetic field, arrangement **b)**, $r = const$*

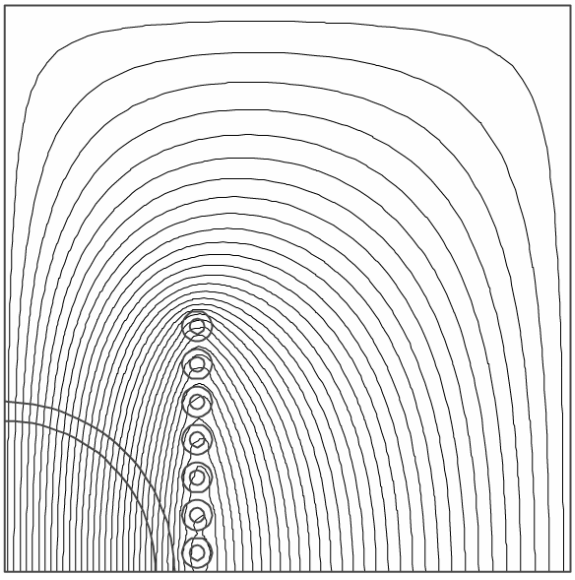

*Fig. 7b. Magnetic field, arrangement **c)**, $x = const$*

For example, Fig. 8a shows that the electric field in channel **1**, arrangement **a)** is strongly uniform (except for small subregions near the corners of the channel – for $x = \pm 0.025$ m, $y = \pm 0.05$ m, see Fig. 2a and also compare Fig. 3). On the other hand, Fig. 8b shows that the electric field in channel **1**, arrangement **b)** is relatively nonuniform and the same holds in case **c)**. The same conclusion can be made, however, even form Figs. 3, 5a and 5b. Comparison of the graphs 8a and 8b moreover says that the vector $\boldsymbol{J}_e$ is greater in case of the arrangement **b)** (the cylindrical channel) and grows with the surfaces of the electrodes (angle α, see Fig. 2b).

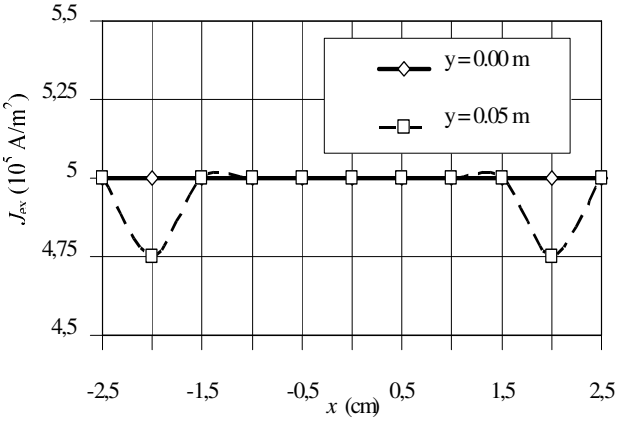

*Fig. 8a. Distribution of the component J_{ex} of vector $\boldsymbol{J}_e$ along the circumference $y = 0$ and $y = 0.05$ mm of channel **1** for arrangement **a)**, $a = 0.05$ mm, see Fig. 2a*

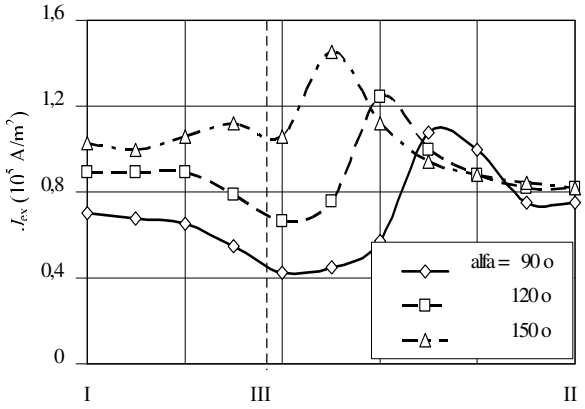

*Fig. 8b. Distribution of the component J_{ex} of vector $\boldsymbol{J}_e$ along the circumference {I-III-II} of channel **1** for arrangement **b)**, see Fig. 2b*

In an analogous way, according to Figs. 9a and 9b it is clear that the magnetic field in channel **1**, arrangement a) is relatively uniform (which is in accordance with Fig. 4), but somewhat weaker than the magnetic field in the channel of the circular cross-section, particularly in the arrangement b) for $r =$ const, compare Fig. 2b.

We may conclude that the most suitable (from the viewpoint of its pumping lead h_L) is the arrangement b) for $r =$ const with the greatest electrodes **2** ($\alpha = 150°$). An analogous conclusion can be derived from the numerical evaluation of integral expression (8), compare the Tabs. 2, 3 and 4. It can be realized, for example, by code

Matlab [9], while the distribution of vectors $\boldsymbol{J}_e$ and $\boldsymbol{B}$ in the cross-section of the channel 1 by code QuickField [6].

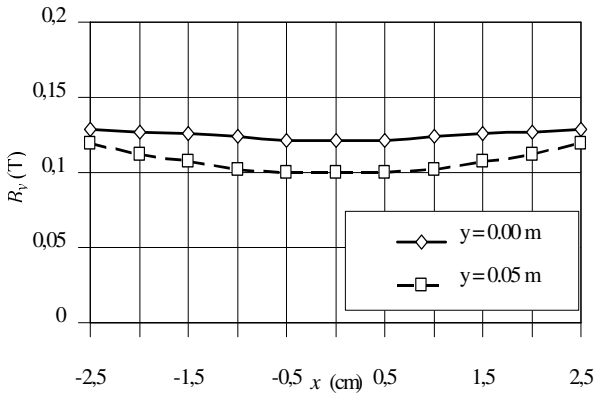

*Fig. 9a. Distribution of the component B_y of vector $\boldsymbol{B}$ along the circumference $y = 0$ and $y = 0.05$ mm of channel **1** for arrangement **a)**, $a = 0.05$ mm, see Fig. 2a*

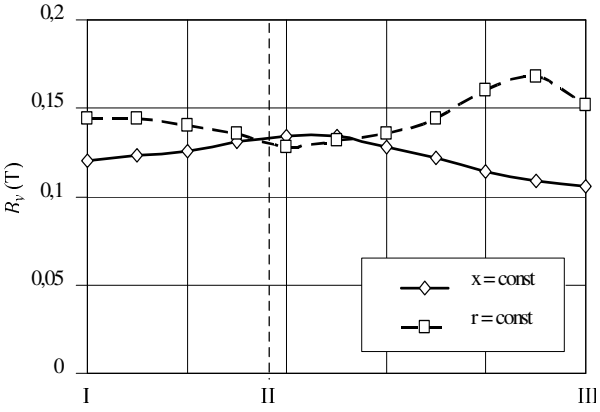

*Fig. 9b. Distribution of the component B_y of vector $\boldsymbol{B}$ along the circumference {I-II-III} of channel **1** for arrangement **b)**, see Fig. 2b*

Tab. 2. Results for the arrangement **a)** for different widths b of the channel

		width of the channel (m) $b = 0.05$	$b = 0.04$	$b = 0.03$
J_{mx}	A/m^2	$5 \cdot 10^5$	$5 \cdot 10^5$	$5 \cdot 10^5$
B_{my}	T	0.12	0.135	0.15
F_{Lz}	N	30.100	26.934	22.453
h_L	m	0.258	0.289	0.321

Tab. 3. Results for the arrangements **b)** for different angles α of the electrodes

		arrangement $r = \text{const}$ $\alpha = 90°$	$\alpha = 120°$	$\boldsymbol{\alpha = 150°}$
J_{mx}	A/m^2	$7.167 \cdot 10^5$	$8.776 \cdot 10^5$	$\mathbf{9.783 \cdot 10^5}$
B_{my}	T	0.143	0.143	**0.143**
F_{Lz}	N	51.244	62.748	**69.948**
h_L	m	0.440	0.539	**0.600**

Tab. 4. Results for the arrangements **c)** for different angles α of the electrodes

		arrangement $x = \text{const}$ $\alpha = 90°$	$\alpha = 120°$	$\alpha = 150°$
J_{mx}	A/m^2	$7.167 \cdot 10^5$	$8.776 \cdot 10^5$	$9.783 \cdot 10^5$
B_{my}	T	0.122	0.122	0.122
F_{Lz}	N	43.719	53.534	59.676
h_L	m	0.375	0.460	0.512

5 CONCLUSION

The analyzed MHD pumps for electrically conductive, nonferromagnetic liquid medium (molten metals, conductive liquids such as acids or electrolytes) represent prospective and technically quite real devices. The presented algorithm makes it possible to find such geometrical and other parameters of the device that satisfies the demands both from the viewpoint of the pumping lead h_L and technological aspects (the shape of the channel, electrodes etc.). It is also necessary to remind that substantial growth of the pumping lead can be achieved by connection of several pumps of this kind in series (from the hydraulic viewpoint) in one working channel.

Next work in the field will be aimed at the experimental verification of conclusions following from the above theoretical analysis.

6 ACKNOWLEDGMENT

Financial support of the Research Plan MSM6840770017, and Grant project GA CR 102/07/0496 is gratefully acknowledged.

7 REFERENCES

[1] S. Kikuchi, K. Murakami, *Behavior of a New DC Electromagnetic Pump Using Superconducting Magnet*, IEEE Trans. Mag. 13, No. 5, 1977, pp. 1559–1561.

[2] N. Takorabet, *Computation of Force Density Inside the Channel of an Electromagnetic Pump by Hermite Projection*, IEEE Trans. Mag. 42, No. 3, 2006, pp. 430–433.

[3] N. Ma, T. J. Moon, J. S. Walker, *Electromagnetic Pump with Thin Metal Walls*, J. Fluid Engrg., Trans. ASME 116, No. 2, 1994, pp. 298–302.

[4] D. Mayer, J. Polak, *Methods of Solution of Electric and Magnetic Fields*, SNTL ALFA, Prague, 1983, in Czech.

[5] L. Hanka, *Theory of Electromagnetic Field*, SNTL ALFA, Prague, 1975, in Czech.

[6] www.quickfield.com.

[7] *Factory Standard SN 006004*, in Czech.

[8] J. Hassdenteufel, K. Kvet, *Materials for Electrical Engineering*, SNTL Praha, 1967, in Czech.

[9] P. Karban, *Computations and Simulations in Codes Matlab and Simulink*, Computer Press, Brno, 2006, in Czech.

Ing. Jiří Bülow, Ing. Pavel Karban, Doc. Ing. Bohuš Ulrych, CSc.
University of West Bohemia
Faculty of Electrical Engineering
Univerzitní 26
306 14 Plzeň
E-mail: {bulow, karban, ulrych}@kte.zcu.cz

Prof. Ing. Ivo Doležel, CSc.
Academy of Sciences of the Czech Republic
Institute of Thermomechanics
Dolejškova 5
182 02 Praha 8
E-mail: dolezel@iee.cas.cz